ACS APPLIED MATERIALS & INTERFACES

Research Article

www.acsami.org

Growth and Proliferation of Human Embryonic Stem Cells on Fully Synthetic Scaffolds Based on Carbon Nanotubes

Eric W. Brunner,[†,‡] Izabela Jurewicz,[†] Elena Heister,[†] Azin Fahimi,[†] Chiara Bo,[†] Richard P. Sear,[†] Peter J. Donovan,[‡] and Alan B. Dalton*[,†]

[†]Department of Physics and Surrey Materials Institute, University of Surrey, Guildford, Surrey GU2 7XH, United Kingdom

[‡]Sue and Bill Gross Stem Cell Research Program, Department of Biological Chemistry, Developmental and Cell Biology Department, Center for Molecular and Mitochondrial Medicine and Genetics, University of California, Irvine, California 92617-1705, United States

Supporting Information

ABSTRACT: Here we show an industrially scalable and inexpensive method of fabricating entirely synthetic, non-xenogeneic carbon nanotube-based scaffolds by vacuum filtration for the culture of human embryonic stem cells. We show that controlled exposure of carbon nanotubes to sonication and the amount of energy delivered to the dispersion directly impacts the surface properties, allowing for control over the nanotopography of the resulting carbon nanotube films, which in turn has demonstrable effects upon in vitro human embryonic stem cells cultures. By altering the nanotube processing conditions before film fabrication, it is possible to influence cell adherence, proliferation and colony morphology. Such a tunable surface with capabilities of influencing stem cell behaviors, combined with the ability to slow or speed population doubling times, will provide crucial solutions for achieving applications envisioned by stem cell biologists to assist future industrial and clinical implementation of human embryonic stem cells.

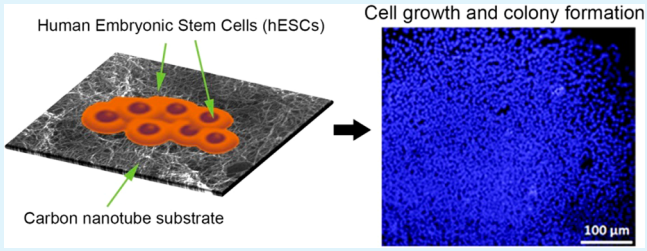

KEYWORDS: *Tissue engineering, human embryonic stem cells, carbon nanotubes, stem cell substrates, pluripotency, biomaterial*

INTRODUCTION

Human embryonic stem cells (hESCs) derived from the inner cell mass of the blastocyst have enormous potential with respect to cell and tissue engineering. Owing to their abilities of self-renewal and differentiation, they can provide an unrestricted source of any human cell type. And because in vitro differentiation of hESCs resembles the early stages of human embryonic development, hESCs are attractive for use in drug discovery and for alternative toxicity testing. Despite the substantial progress being made since the isolation and growth of the first hESC line in 1998, several obstacles still exist before such applications can be realized. Stem cells tend to spontaneously differentiate in culture, which rapidly reduces the number of multipotent cells and their regenerative capacity. Furthermore, most conventional substrates, such as Matrigel or a co-culture with feeder cells, can impart pathogens, elicit immunogenic responses, and often display batch-to-batch variety. Hence, there is a strong need for a growth scaffold that is non-xenogeneic and provides industrial scalability, batch-to-batch reliability, and tunability of physiochemical and biological surface cues to promote long-term self-renewal.

Moreover, it is becoming gradually more evident that all mammalian cells in general are environmentally sensitive and will respond to various surface properties of their underlying substrates[1,2] including roughness,[3] wettability,[4] substrate stiffness,[5,6] surface chemistry,[7] and in some cases conductivity[8] or electrical stimulation.[9] Carbon nanotubes (CNTs) as a scaffold material have considerable potential to meet the complexities of hESC culture systems: their nanosized dimensions and fibrillar shape closely resembles the topography of the extracellular matrix[10] and their surface chemistry is easily modified, allowing for functionalization with biological signaling molecules[11] or controlled release of growth factors.[12] CNT-based scaffolds for cell culture have been successfully fabricated by a variety of methods including forest drawing,[13] electrospinning of nanofibers,[14,15] solvent casting,[16] and incorporation into composites.[17−20]

Although these nanostructured materials have been extensively used in the field of biomedicine, their use in hESCs has not been significantly explored. Chao et al.[21] showed that a 2D scaffold composed of biocompatible polymer grafted CNTs can selectively differentiate human embryonic stem cells into neuron cells while maintaining excellent cell viability. A similar result was obtained by Sebaa et al.[22] on graphene and Multiwall carbon nanotubes (MWNT)−graphene hybrids fabricated using chemical vapor deposition (CVD). Another study showed

Received: November 13, 2013
Accepted: January 21, 2014
Published: January 23, 2014

that silk−CNT-based composite scaffolds can effectively promote neuronal differentiation of hESCs.[23]

Here we show an industrially scalable and inexpensive method for fabricating entirely synthetic, non-xenogeneic CNT-based thin films by vacuum filtration for the culture of hESCs. We show that controlled exposure of CNTs to sonication and the amount of energy delivered to the dispersion directly impacts the surface properties allowing for control over the nanotopography of the resulting CNT films, which in turn has demonstrable effects upon in vitro hESC cultures. By altering the nanotube processing conditions before film fabrication, it is possible to influence cell adherence, proliferation, and colony morphology. Such a tunable surface with capabilities of influencing stem cell behaviors, combined with the ability to slow or speed population doubling times will provide crucial solutions for achieving applications envisioned by stem cell biologists.

EXPERIMENTAL SECTION

NH_2−MWNT Film Fabrication. Three types of NH_2−MWNT dispersions were prepared by bath sonication (275 W output power) of 5 mg of as-received NH_2−MWNTs (Nanocyl, Belgium) in 500 mL of Milli-Q water for 5, 60, and 300 min respectively. The chemical reactions Nanocyl employs to functionalize MWCNTs proceed first by acid oxidation treatment to attach carboxylic acid groups to MWCNT sidewall and then by the Schmidt reaction that produces an approximately half and half mixture of resulting amine and amide organic groups.[24] The total amount of energy (E) delivered to a CNT dispersion depends on the applied power (P) and on the total amount of time (t) that the dispersion is subject to the ultrasonic treatment and can be calculated using following equation: $E = P \times t$ (Table 1) given below:

Table 1. Calculated Energy Delivered to the CNT Dispersion Based on Applied Output Power and Sonication Time

sample name	output power P (W)	sonication time t (min)	energy delivered E (kJ)
$MWNT_{80}$	275	5	88
$MWNT_{1000}$	275	60	990
$MWNT_{5000}$	275	300	4950

To fabricate NH_2−MWNT thin films, immediately following sonication, 50 mL of each dispersion was vacuum-filtered using mixed nitrocellulose membranes (Millipore) with 0.22 μm average pore sizes These were allowed to settle and dried at 70 °C for 6 h. CNT films were then transferred from a membrane filter to the glass substrate by dissolving the filter in acetone. Briefly, a nitrocellulose filter with a MWNT thin film was placed on the glass coverslip with the MWNT contacted the top surface of the substrate. The resulting filter-attached substrate was dissolved by repeated immersion in acetone and finally methanol. It was necessary to fabricate our substrates with thicknesses exceeding several micrometers to ensure mechanical integrity once the supporting membrane was removed.

Investigation of Substrate Morphology. Microstructural investigations of MWNT thin films were done using a FEI Quanta 200 scanning electron microscope (SEM) at an accelerating voltage of 30 kV, a working distance of 6−10 mm, and a spot size of 2 nm. Owing to the relatively high electrical conductivity of the samples, they were imaged without sputtering a metal onto their surface. Several spots of each microscope sample, prepared with the same CNT dispersion after respectively 5, 60, and 300 min of sonication, were checked and imaged. For topographic studies and surface roughness analysis, an atomic force microscope (AFM) (NT-MDT, Moscow, Russia), using semicontact mode, was employed. The AFM probes (NT-MDT) had an average spring constant of 11.8 N/m. Ten 40 × 40 μm scan areas recorded with resolutions of 256 × 256 points were sampled on each of the three surfaces and analyzed by Nova 959 image analysis software (NT-MDT). The roughness of each scanned surface area is defined by

$$R = \frac{1}{n}\sum_{i=0}^{n} |y_i|$$

where R is the roughness, n is the number of points, and y_i is the difference between the height of an individual point and the average height for every point within the scan.

Static contact angle measurements were performed with an automated tensiometer (Krüss EasyDrop Standard DSA15). Then 2.5 μL droplets of Milli-Q water were dispensed onto MWNT surfaces using a microsyringe and captured with a monochrome interline CCD camera. Five measurements were performed on each NH_2−MWNT surface, and images were analyzed using the Tangent Method 2 in the accompanying DSA 1 software.

Stem Cell Culture. H9 hESC cell lines (passages 43−51) were cultured in 80% DMEM-F12 (Gibco), 20% KNOCKOUT serum replacement (Gibco), 1 mM L-glutamine (Gibco), 0.1 mM β-mercaptoethanol (Fisher), 1% nonessential amino acids (Gibco), and 4 ng/mL of human basic fibroblast growth factor (R&D systems) and passaged regularly approximately every 5 days before reaching confluency. hESCs were plated at densities of ∼1,000 cells/cm^2 in co-culture with mouse embryonic feeders (Chemicon) plated at densities of ∼200 cells/cm^2. For cultures on Matrigel (BD Falcon), Matrigel solutions were thawed overnight on ice at 4 °C, diluted in DMEM-F12, and then deposited onto tissue culture dishes in cellular incubators at standard conditions for 1 h. For cultures on NH_2−MWNT films (transferred to glass coverslips as described above), the films and coverslips were autoclaved before use in cell culture.

Immunocytochemistry. Colonies were fixed 5 days after plating in 4% paraformaldehyde for 15 min, treated for 5 min in 0.05% Triton X-100 in PBS, and washed three times with PBS. Antibodies to Oct-4 and SSEA-4 were obtained from R&D Systems, and antibodies to TRA-1-81 were obtained from Millipore. Antibodies were diluted in blocking buffer containing 10% heat-inactivated serum from the same species as the secondary antibody and 0.01% Triton-X in PBS and used to treat the colonies overnight at 4 °C. Colonies were washed three times with PBS. FITC or TRITC conjugated secondary antibodies were diluted in the same blocking buffer and used to treat the colonies for 1 h. Colonies were washed three times with PBS and then immediately imaged.

AP staining. Fixed hESC samples were washed three times with Milli-Q water. Fast Red reagent (Invitrogen) was dissolved in Milli-Q water at a concentration of 1 mg/mL, and 40 μL of napthol phosphate buffered solution (Invitrogen) was added to every 1 mL of the Fast Red solution immediately before addition to fixed hESC samples. Samples were immersed in the staining solutions until the bright red precipitate formed on the cellular surfaces and were then washed three times with Milli-Q water.

Viability and Proliferation. Colonies were treated with 0.05% trypsin-EDTA, collected with two washings of standard hESC media and centrifuged at 1000 rcf. The supernatant was decanted without disturbing the cell pellet, and equal volumes of 0.4% Tryphan Blue Stain (Invitrogen) were added to the sediment. Viable and nonviable cells were counted ten times for each sample using a hemocytometer. Samples were tested in triplicate.

RESULTS AND DISCUSSION

Multiwall carbon nanotubes (MWNTs) functionalized with amino groups (NH_2) were chosen for this work to avoid the use of surfactants or high-boiling point organic solvents commonly used in CNT processing, which are often toxic to cells. In addition, removal of such agents would require additional processing of the CNT films under extreme annealing conditions or washing the films in copious volumes of solvent, which would still not guarantee the complete

removal of trace contaminants that may later give rise to undesirable complications with hESC cultures. NH_2 groups were given preference over the commonly employed carboxylic acid functionalization scheme on account of previously reported cell culture affinities for positively charged surfaces.[25,26]

It is well known that the CNT bundle polydispersity in size decreases with increasing sonication time, because the total amount of energy (E) delivered to the CNT dispersion is directly proportional to the applied power (P) and the total amount of sonication time (t), respectively. As can be seen in Figure 1a, the absorbance of a CNT dispersion increases with

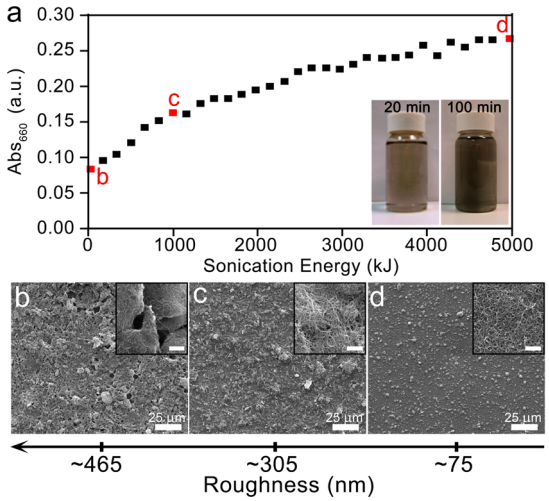

Figure 1. (a) Absorbance at 660 nm as a function of sonication energy for an aqueous NH_2−MWNT dispersion, showing an increase in absorption with sonication exposure corresponding to the debundling of MWNT aggregates. (a−c) SEM images of MWNT surfaces with varying roughness made from dispersions exposed to sonication energies of (b) 80 kJ, (c) 1000 kJ, and (d) 5000 kJ, respectively. (Insets: high magnification SEM images showing local morphology. Scale bar = 500 nm).

added sonication exposure and serves as an indicator of the dispersion's aggregation state, as more individualized CNTs are released into solution with time.

For the fabrication of MWNT films, three dispersions of MWNTs were used after 5 ($MWNT_{80}$), 60 ($MWNT_{1000}$), and 300 ($MWNT_{5000}$) min of sonication (corresponding to energy inputs of ~80, ~1000, and ~5000 kJ, respectively), as indicated in Figure 1. The first dispersion ($MWNT_{80}$) was taken directly at the beginning of the debundling process, thus black CNT aggregates are still visible by the naked eye. On the basis of UV−vis spectroscopy, after 60 min of sonication, aggregates and big CNT ropes are present in the dispersion but a large fraction of CNTs has already been exfoliated and individualized. The third dispersion was taken after 300 min of sonication where CNTs are mostly isolated. Immediately following sonication, films of NH_2−MWNTs of various roughnesses were fabricated using three types of dispersions described above. During vacuum filtration, individualized MWNTs, as well as aggregates within the dispersion, were deposited upon filter membranes, thereby directly affecting the topography of the resulting film's surface. Obvious trends exist between the dispersion aggregation state and the surface properties of resulting MWNT films fabricated from dispersions exposed to different sonication energies, as shown in Figure 1b−d. Figure 1b distinctively shows big aggregates of NH_2−MWNTs that become significantly reduced by increasing the sonication energy (Figure 1 c,d), resulting in the change of the substrate's micro- and macro-scale morphology, while maintaining the nanoscale morphology as unaltered.

The surface roughness of resulting films was measured by atomic force microscopy (AFM) (Supporting Information, Figure S1). Ten 40 × 40 μm AFM scans over each type of surface revealed that both average roughness and standard deviation over the ten scans decreased with increasing sonication energy: the surface roughness was found to be 467 ± 56 nm for $MWNT_{80}$ films, 308 ± 54 nm for $MWNT_{1000}$ films, and 75 ± 15 nm for $MWNT_{5000}$ films. Static contact angle measurements demonstrated these as-produced MWNT surfaces to be hydrophobic, but because hydrophobic surfaces are known to be poor candidates for cell substrates in general, we tested the wettability of these surfaces following immersion in growth media for 1 h under the assumption that media components would absorb onto the MWNTs' sidewalls. We observed that water droplets immediately absorbed onto $MWNT_{80}$ films and $MWNT_{1000}$ films and, within a matter of minutes, also onto $MWNT_{5000}$ films. The immediate absorption of the water droplet onto $MWNT_{80}$ and $MWNT_{1000}$ films, as opposed to the gradual absorption of the droplet onto $MWNT_{5000}$ films, can be attributed to the presence of macropores within $MWNT_{80}$ and $MWNT_{1000}$ films that are absent in $MWNT_{5000}$ films.

The responses of hESCs to the three different MWNT surfaces in terms of the number of adhered cells and resulting colony morphologies were evaluated. Figure 2 shows that significantly decreased numbers of cells adhered onto the $MWNT_{1000}$ and $MWNT_{5000}$ films compared to $MWNT_{80}$ films, indicating that hESCs prefer rough surfaces to smooth ones. This is in good agreement with previous study, which showed that human mesenchymal stem cells (hMSCSs) spread better on a single-walled carbon nanotube (SWNT) film with a roughness of about 100 nm than on a coverslip and had a higher occurrence of filopodia.[10] The authors of the latter study hypothesize that this could be due to the limited surface area of an individual nanotube combined with the random spacing between fibers, which could restrict the formation of focal adhesions and large stress fibers necessary for cell attachment. Overall, the cell adhesion is strongly influenced by the surface roughness and varies between different cell types. It remains to be elucidated whether an optimal roughness for stem cell culture exists, as has been found for a culture of osteoblasts, which showed robust spreading at a surface roughness of about 100 nm but less spreading and cytoplasmic extensions on smoother and rougher substrates.[27]

We next investigated the colony morphology on $MWNT_{80}$ and $MWNT_{1000}$ films after seeding. It was found that colonies on $MWNT_{80}$ films grew to standard sizes and possessed a flattened morphology compared to colonies on $MWNT_{1000}$ films, which exhibited smaller sizes and clustered morphologies, as shown in Figure 2. No colonies remained on $MWNT_{5000}$ films on day five after plating, as they were washed away with daily media changes. This spheroid colony morphology on $MWNT_{1000}$ films is easily visualized in fluorescent images by depicting the cell nuclei within a colony

Figure 2d shows a fluorescent image with a highly condensed colony center corresponding to the clustered morphology with single layer cells protruding outward around the periphery. These centers are present on some colonies on $MWNT_{80}$ but

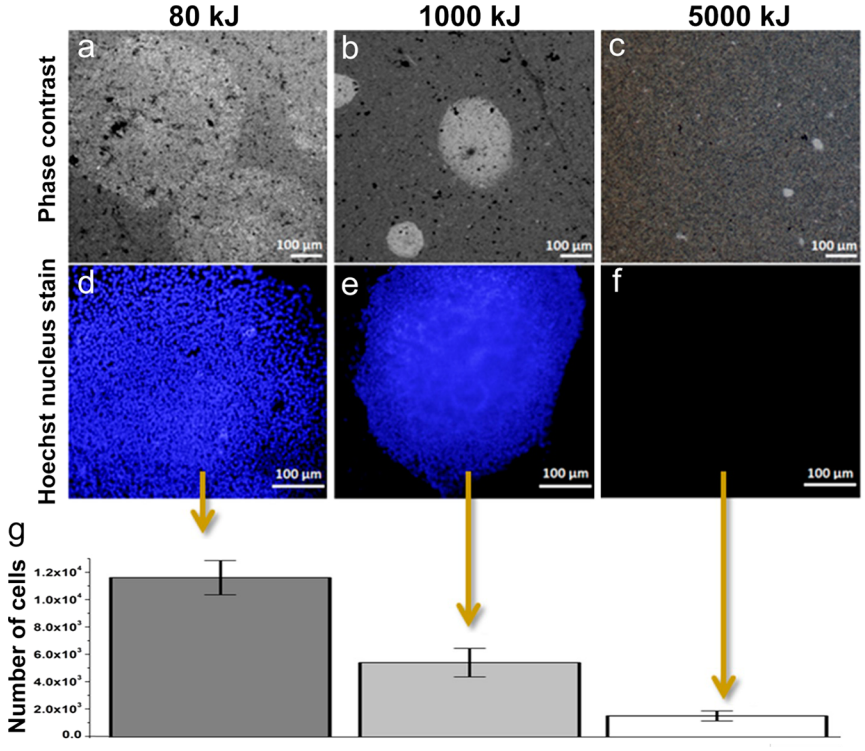

Figure 2. Comparison of cellular behaviors on different MWNT surfaces relative to the dispersion sonication energy. (a–c) Phase contrast and (d–f) Hoechst nucleus staining of stem cell colonies, demonstrating no adherences of colonies after 36 h for $MWNT_{5000}$ films, colonies with clustered morphologies and limited expansion on $MWNT_{1000}$ films after 120 h and densely packed colonies demonstrating expansive growth on $MWNT_{80}$ also after 120 h. (g) Number of adhered cells after 36 h for $MWNT_{80}$, $MWNT_{1000}$, and $MWNT_{5000}$ (n = 3).

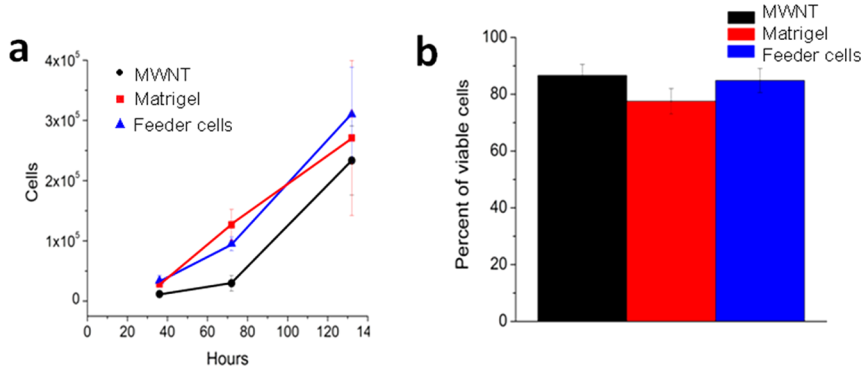

Figure 3. Comparison between colonies grown on optimized $MWNT_{80}$, Matrigel, and feeders and retention of pluripotent markers. (a) Growth curve showing total number of cells at 36, 72, and 132 h (n = 3). Bars, standard deviation of n = 3 samples. (b) Percentage of viable cells on day five following plating (n = 3).

are significantly reduced compared to every hESC colony on $MWNT_{1000}$. Stacking of cells on top of other cells, as observed here, qualitatively implies weak cell-surface interactions and a scarcity of favorable contact points with $MWNT_{1000}$ films. These results for adherence and morphology suggest that hESC colonies have affinities for microstructures composed of MWNTs, macropores, or both, as either surface feature may provide the traction necessary for colony expansion.

$MWNT_{80}$ films yielded the most promising results of the three tested MWNT films and were further tested in subsequent trials against conventional substrates, including a co-culture of mouse embryonic fibroblasts (MEFs) and a surface coating layer rich in extracellular matrix (ECM) proteins, referred to as Matrigel.

Colonies on $MWNT_{80}$ were evaluated to those grown in co-culture with MEFs or on Matrigel in terms of adhesion, proliferation, and expression of pluripotent markers. Figure 3a displays a growth curve for the three tested substrates over a six day period and shows that the number of cells adhered onto $MWNT_{80}$ at 36 and 72 h after plating are lower than the number of adhered cells on either biological substrate; however, the number of cells present at 132 h after plating was not significantly different from the number of cells grown on either MEFs or Matrigel. This delay in proliferation of cells grown on $MWNT_{80}$ may be attributed to the possibility that hESCs first need to condition the MWNT surface through excretion of ECM proteins to modify the surface before proliferation can increase.

dx.doi.org/10.1021/am405097w | ACS Appl. Mater. Interfaces 2014, 6, 2598–2603

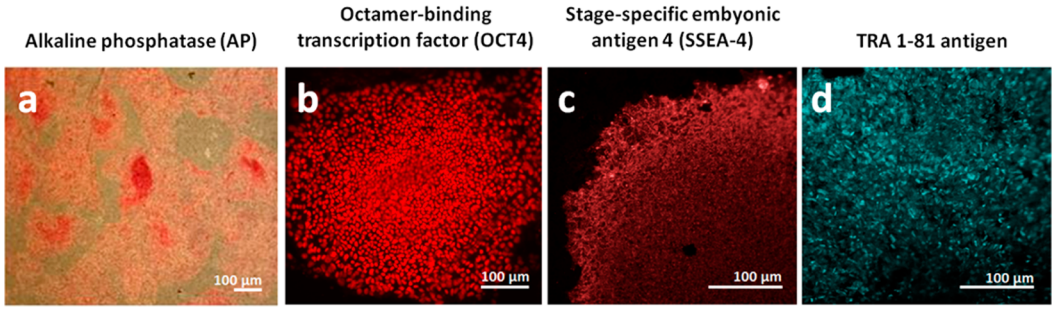

Figure 4. Colonies on day five after plating stained with pluripotent markers alkaline phosphatase (a), OCT4 (b), SSEA-4 (c), and TRA-1-81 (d).

Cellular viability was assessed by the Tryphan Blue assay at 72 (Supporting Information, Figure S2) and 132 h (Figure 4b) after plating and no significant statistical difference was observed among any of the three substrates. This demonstrates that $MWNT_{80}$ films are entirely sufficient to replace the standard hESC biological substrates in terms of proliferation and viability.

Unless the aim is to direct hESCs to differentiate into a specific cell type, hESCs must also retain their abilities to differentiate into the majority of all other cell types, termed as pluripotency. Expression levels of certain biological markers diminish over time as hESCs begin to permanently differentiate into other cell types; therefore, a viable hESC substrate must also be assessed as to the effects it may impose upon hESC pluripotency, as other substrates have demonstrated the ability to influence the differentiation behaviors of stem cells.[28,29] On day five, after plating, hESCs grown on $MWNT_{80}$ were evaluated in terms of their expression of standard pluripotent markers including alkaline phosphatase, stage-specific embryonic antigen (SSEA-4), TRA 1-81 antigen, and octamer-binding transcription factor (OCT4).

Figure 4a shows a brightfield image of hESCs grown on $MWNT_{80}$ films stained with alkaline phosphatase marker that imparts a bright red precipitate upon the cell surface, signifying the presence of the membrane enzyme. Similarly, Figure 4b,c,d shows the fluorescent images of colonies grown on $MWNT_{80}$ films immunostained with OCT4, SSEA-4, and TRA-1-81 captured at equal or lesser exposure times than colonies grown on MEFs (Supporting Information, Figure S3). It should be noted that some of the colonies begin to show uneven edges. Such morphology may indicate the onset of differentiation, which is not uncommon as colonies get larger.

These results qualitatively demonstrate equal expression levels of conventional pluripotent markers for hESCs grown on both $MWNT_{80}$ films or MEFs, evidencing that $MWNT_{80}$ has no apparent immediate stimulatory effects upon hESC differentiation. This is in agreement with a study by Akasaka et al., which demonstrated that thick films of MWNTs supported the maintenance of highly undifferentiated mouse induced pluripotent stem cells for 5 days.[30]

CONCLUSIONS

Taken together, these results covering proliferation, viability, and expression of pluripotent markers demonstrate the potential for CNT thin films to compete with conventional hESC substrates and add to the growing interest of CNT constructs to serve as substrates for specialized cell types. Given the simplicities of our scaffold fabrication method and tunability of the MWNT surface properties, one can easily envision numerous applications of CNT-assisted biomaterials tailored for the many challenges hESC biologists face. This is particularly relevant when considering advanced variations of CNT constructs with embedded growth factors, covalently-attached synthetic RGD binding peptides, and other signaling cues, which will further aid not only the growth of in vitro cell cultures but also cells seeded into 3D constructs for tissue implantation therapies. Such functionalization strategies combined with some of the inherent physical characteristics of CNTs, including conductivity, aspect ratio, high-tensile strength, and actuation, may find unique roles for tempering growth rates, electrically innervating attached cells, kinetically controlling the release of growth factors, and directing the differentiation or self-renewal behaviors of hESCs, to name a few. Finally, the scalability of our film fabrication process speaks to the readiness of CNTs to assist industrial and clinical applications of hESCs.

ASSOCIATED CONTENT

Supporting Information

AFM height images of MWNT films fabricated from dispersions exposed to different sonication energies, percentage of viable cells assessed by the Tryphan Blue assay at 72 h after plating for hESCs grown various substrates as well as images of colonies on day five after plating stained with various pluripotent markers. This material is available free of charge via the Internet at http://pubs.acs.org.

AUTHOR INFORMATION

Corresponding Author

* Dr. Alan B. Dalton. E-mail: a.dalton@surrey.ac.uk. Phone: +44 1483 68 6787.

Author Contributions

The paper was written through contributions of all authors. All authors have given approval to the final version of the paper.

Notes

The authors declare no competing financial interest.

ACKNOWLEDGMENTS

The authors gratefully acknowledge financial support from Human Frontier Science Program, Royal Society, Engineering and Physical Sciences Research Council, SETsquared, and Beckman Coulter Inc.

REFERENCES

(1) Roach, P.; Eglin, D.; Rohde, K.; Perry, C. C. Modern biomaterials: a review-bulk properties and implications of surface modifications. *J. Mater. Sci.: Mater. Med.* **2007**, *18*, 1263−1277.

(2) Lee, M. R.; Kwon, K. W.; Jung, H.; Kim, H. N.; Suh, K. Y.; Kim, K.; Kim, K.-S. Direct differentiation of human embryonic stem cells

into selective neurons on nanoscale ridge/groove pattern arrays. *Biomaterials* **2010**, *31*, 4360−4366.
(3) Mwenifumbo, S.; Shaffer, M. S.; Stevens, M. M. Exploring cellular behaviour with multi-walled carbon nanotube constructs. *J. Mater. Chem.* **2007**, *17*, 1894−1902.
(4) Moon, S. U.; Kim, J.; Bokara, K. K.; Kim, J. Y.; Khang, D.; Webster, T. J.; Lee, J. E. Carbon nanotubes impregnated with subventricular zone neural progenitor cells promotes recovery from stroke. *Int. J. Nanomed.* **2012**, *7*, 2751−2765.
(5) Mih, J. D.; Sharif, A. S.; Liu, F.; Marinkovic, A.; Symer, M. M.; Tschumperlin, D. J. A Multiwell Platform for Studying Stiffness-Dependent Cell Biology. *PLoS One* **2011**, *6*, e 19929.
(6) Eroshenko, N.; Ramachandran, R.; Yadavalli, V.; Rao, R. Effect of substrate stiffness on early human embryonic stem cell differentiation. *J. Biol. Eng.* **2013**, *7*, 7.
(7) Phillips, J. E.; Petrie, T. A.; Creighton, F. P.; Garcia, A. J. Human mesenchymal stem cell differentiation on self-assembled monolayers presenting different surface chemistries. *Acta Biomater.* **2010**, *6*, 12−20.
(8) Cellot, G.; Cilia, E.; Cipollone, S.; Rancic, V.; Sucapane, A.; Giordani, S.; Gambazzi, L.; Markram, H.; Grandolfo, M.; Scaini, D.; Gelain, F.; Casalis, L.; Prato, M.; Giugliano, M.; Ballerini, L. Carbon nanotubes might improve neuronal performance by favouring electrical shortcuts. *Nat. Nanotechnol.* **2009**, *4*, 126−133.
(9) Supronowicz, P. R.; Ajayan, P. M.; Ullmann, K. R.; Arulanandam, B. P.; Metzger, D. W.; Bizios, R. Novel current-conducting composite substrates for exposing osteoblasts to alternating current stimulation. *J. Biomed. Mater. Res.* **2002**, *59*, 499−506.
(10) Tay, C. Y.; Gu, H. G.; Leong, W. S.; Yu, H. Y.; Li, H. Q.; Heng, B. C.; Tantang, H.; Loo, S. C. J.; Li, L. J.; Tan, L. P. Cellular behavior of human mesenchymal stem cells cultured on single-walled carbon nanotube film. *Carbon* **2010**, *48*, 1095−1104.
(11) Kam, N. W. S.; O'Connell, M.; Wisdom, J. A.; Dai, H. J. Carbon nanotubes as multifunctional biological transporters and near-infrared agents for selective cancer cell destruction. *Proc. Natl. Acad. Sci. U. S. A.* **2005**, *102*, 11600−11605.
(12) Thompson, B. C.; Moulton, S. E.; Gilmore, K. J.; Higgins, M. J.; Whitten, P. G.; Wallace, G. G. Carbon nanotube biogels. *Carbon* **2009**, *47*, 1282−1291.
(13) Abdullah, C. A. C.; Asanithi, P.; Brunner, E. W.; Jurewicz, I.; Bo, C.; Azad, C. L.; Ovalle-Robles, R.; Fang, S.; Lima, M. D.; Lepro, X.; Collins, S.; Baughman, R. H.; Sear, R. P.; Dalton, A. B. Aligned, isotropic and patterned carbon nanotube substrates that control the growth and alignment of Chinese hamster ovary cells. *Nanotechnology* **2011**, *22*, 205102.
(14) Han, Z.; Kong, H.; Meng, J.; Wang, C.; Xie, S.; Xu, H. Electrospun Aligned Nanofibrous Scaffold of Carbon Nanotubes-Polyurethane Composite for Endothelial Cells. *J. Nanosci. Nanotechnol.* **2009**, *9*, 1400−1402.
(15) Liao, H.; Qi, R.; Shen, M.; Cao, X.; Guo, R.; Zhang, Y.; Shi, X. Improved cellular response on multiwalled carbon nanotube-incorporated electrospun polyvinyl alcohol/chitosan nanofibrous scaffolds. *Colloids Surf., B* **2011**, *84*, 528−535.
(16) Cheng, Q.; Rutledge, K.; Jabbarzadeh, E. Carbon Nanotube−Poly(lactide-co-glycolide) Composite Scaffolds for Bone Tissue Engineering Applications. *Ann. Biomed. Eng.* **2013**, *41*, 904−916.
(17) Shi, X.; Hudson, J. L.; Spicer, P. P.; Tour, J. M.; Krishnamoorti, R.; Mikos, A. G. Rheological behaviour and mechanical characterization of injectable poly(propylene fumarate)/single-walled carbon nanotube composites for bone tissue engineering. *Nanotechnology* **2005**, *16*, S531.
(18) Edwards, S. L.; Church, J. S.; Werkmeister, J. A.; Ramshaw, J. A. M. Tubular micro-scale multiwalled carbon nanotube-based scaffolds for tissue engineering. *Biomaterials* **2009**, *30*, 1725−1731.
(19) Abarrategi, A.; Gutiérrez, M. C.; Moreno-Vicente, C.; Hortigüela, M. J.; Ramos, V.; López-Lacomba, J. L.; Ferrer, M. L.; del Monte, F. Multiwall carbon nanotube scaffolds for tissue engineering purposes. *Biomaterials* **2008**, *29*, 94−102.
(20) Zawadzak, E.; Bil, M.; Ryszkowska, J.; Nazhat, S. N.; Cho, J.; Bretcanu, O.; Roether, J. A.; Boccaccini, A. R. Polyurethane foams electrophoretically coated with carbon nanotubes for tissue engineering scaffolds. *Biomed. Mater.* **2009**, *4*, 015008.
(21) Chao, T.-I.; Xiang, S.; Chen, C.-S.; Chin, W.-C.; Nelson, A. J.; Wang, C.; Lu, J. Carbon nanotubes promote neuron differentiation from human embryonic stem cells. *Biochem. Biophys. Res. Commun.* **2009**, *384*, 426−430.
(22) Sebaa, M.; Nguyen, T. Y.; Paul, R. K.; Mulchandani, A.; Liu, H. Graphene and carbon nanotube−graphene hybrid nanomaterials for human embryonic stem cell culture. *Mater. Lett.* **2013**, *92*, 122−125.
(23) Chen, C.-S.; Soni, S.; Le, C.; Biasca, M.; Farr, E.; Chen, E.; Chin, W.-C. Human stem cell neuronal differentiation on silk-carbon nanotube composite. *Nanoscale Res. Lett.* **2012**, *7*, 126.
(24) Wade, L. G. *Organic chemistry*; Prentice Hall: Upper Saddle River, NJ, 1999.
(25) Rainaldi, G.; Calcabrini, A.; Santini, M. T. Positively charged polymer polylysine-induced cell adhesion molecule redistribution in K562 cells. *J. Mater. Sci.: Mater. Med.* **1998**, *9*, 755−760.
(26) Hu, H.; Ni, Y. C.; Montana, V.; Haddon, R. C.; Parpura, V. Chemically functionalized carbon nanotubes as substrates for neuronal growth. *Nano Lett.* **2004**, *4*, 507−511.
(27) Tutak, W.; Chhowalla, M.; Sesti, F. The chemical and physical characteristics of single-walled carbon nanotube film impact on osteoblastic cell response. *Nanotechnology* **2010**, *21*, 315102.
(28) Sridharan, I.; Kim, T.; Wang, R. Adapting collagen/CNT matrix in directing hESC differentiation. *Biochem. Biophys. Res. Commun.* **2009**, *381*, 508−512.
(29) Engler, A. J.; Sen, S.; Sweeney, H. L.; Discher, D. E. Matrix elasticity directs stem cell lineage specification. *Cell* **2006**, *126*, 677−689.
(30) Akasaka, T.; Yokoyama, A.; Matsuoka, M.; Hashimoto, T.; Watari, F. Maintenance of hemiround colonies and undifferentiated state of mouse induced pluripotent stem cells on carbon nanotube-coated dishes. *Carbon* **2011**, *49*, 2287−2299.